THE BOUNDARY LAYERS OF A FULLY IONIZED TWO-TEMPERATURE PLASMA WITH GIVEN COMPONENT TEMPERATURES AT AN ELECTRODE

V. M. Korovin

UDC 532.526+538.4

The flow of a plasma with different component temperatures in the boundary layers at the electrodes of an MHD channel is investigated without any assumptions as to self-similarity. For the calculation of the electron temperature, the full energy equation for an electron gas [1] is solved with allowance for the estimates given in [2]. In contrast to [3, 4], the calculation includes the change in temperature of electrons and ions along the channel caused by the collective transport of energy, the work done by the partial pressure forces, and the Joule heating and the energy exchange between the components. The problem of the boundary layers in the flow of a two-temperature, partially ionized plasma past an electrode is solved in simplified form by the local similarity method in [5-7]. In these papers, either the Kerrebrock equation is used [5, 6] or the collective terms are omitted from the electron energy equation [7].

1. Initial Equations

We consider the flow of a plasma with different component temperatures in a plane channel $0<x<L=$ const, $0<y<a=$const formed by two parallel electrodes $y=0$ and $y=a$. An external potential difference is applied between the electrodes such that the wall $y=0$ is the anode and the wall $y=a$ is the cathode. The plasma enters the channel in such a way that its parameters are constant over a cross section. It is assumed that there is a homogeneous magnetic field $H=(0, 0, H)$.

We consider the case when the gradients of velocity and temperature in the center of the flow are small compared with those near the electrodes so that the flow can be divided into an external flow of a nonviscous and nonthermally conducting medium and narrow boundary layers in which viscosity and thermal conduction play a significant role. It is assumed that the potential drop in the boundary layers is small compared to the potential difference between the electrodes. The system of MHD equations for the boundary layer in a two-temperature plasma has the form [2]

$$\frac{\partial \rho v_x}{\partial x}+\frac{\partial \rho v_y}{\partial y}=0, \quad p_\delta=p_e+p_i, \quad p_e=n_e T_e, \quad p_i=n_i T_i \tag{1.1}$$

$$\rho v_x \frac{\partial v_x}{\partial x}+\rho v_y \frac{\partial v_x}{\partial y}=-\frac{d p_\delta}{d x}+\frac{\partial}{\partial y}\left(\mu_i \frac{\partial v_x}{\partial y}\right)+\frac{1}{c} j_{y\delta} H \tag{1.2}$$

$$\frac{5}{2} n_i v_x \frac{\partial T_i}{\partial x}+\frac{5}{2} n_i v_y \frac{\partial T_i}{\partial y}=\frac{\partial}{\partial y}\left(\varkappa_i \frac{\partial T_i}{\partial y}\right)+\mu_i\left(\frac{\partial v_x}{\partial y}\right)^2+v_x \frac{\partial p_i}{\partial x}+v_y \frac{\partial p_i}{\partial y}+\gamma\left(T_e-T_i\right) \tag{1.3}$$

$$\frac{5}{2} n_e v_x \frac{\partial T_e}{\partial x}+\frac{5}{2} n_e v_y \frac{\partial T_e}{\partial y}=\frac{\partial}{\partial y}\left(\varkappa_e \frac{\partial T_e}{\partial y}\right) \pm \frac{5}{2e} j_{y\delta} \frac{\partial T_e}{\partial y}+v_x \frac{\partial p_e}{\partial x}+v_y \frac{\partial p_e}{\partial y} \mp \frac{1}{e n_e} \frac{\partial p_e}{\partial y}+\frac{j_{y\delta}^2}{\sigma}-\gamma\left(T_e-T_i\right) \tag{1.4}$$

Moscow. Translated from Zhurnal Prikladnoi Mekhaniki i Tekhnicheskoi Fiziki, No. 5, pp. 3-10, September-October, 1972. Original article submitted April 13, 1972.

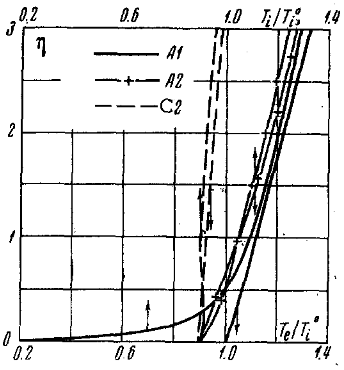

Fig. 1

$$j_{y\delta} = \sigma_\delta (E_{y\delta} - c^{-1} v_{x\delta} H), \quad E_{y\delta} = \text{const}, \quad H = \text{const} \tag{1.5}$$

$$\mu_i = 0.96 n_i T_i \tau_i, \quad \varkappa_i = \frac{3.906 n_i T_i \tau_i}{m_i}, \quad \varkappa_e = \frac{3.1616 n_e T_e \tau_e}{m_e}$$

$$\sigma = \frac{e^2 n_e \tau_e}{0.5129 m_e}, \quad \tau_e = \frac{3}{4}\sqrt{\frac{m_e}{2\pi}}\frac{T_e^{3/2}}{\lambda e^4 n_i}, \quad \tau_i = \frac{3}{4}\sqrt{\frac{m_i}{\pi}}\frac{T_i^{3/2}}{\lambda e^4 n_i}$$

$$\lambda = \ln\left(\frac{3}{4e^3}\sqrt{\frac{T_e T_i (T_e + T_i)}{\pi n_e}}\right), \quad \gamma = \frac{3 m_e}{m_i}\frac{n_e}{\tau_e}$$

Here $\mathbf{v} = (v_x, v_y)$ is the average mass velocity; E_y is the strength of the transverse electric field; j_y is the projection of the current density on to the external normal to the anode surface; T_k, n_k are the temperature and number per unit volume of particles of the k-th kind; p, p_k are the total and partial pressures; m_k, τ_k are the mass of the particles and the time between collisions among particles of the same kind; $\rho = m_e n_e + m_i n_i \approx m_i n_i$ is the plasma density; σ is the conductivity; e, m_p are the charge and mass of a proton; c is the velocity of light. The subscript e denotes quantities refering to electrons, and i those refering to ions; the subscript δ refers to the external flow, 0 to the channel input parameters, and w to the electrodes. We note that the terms $2.5e^{-1} j_{y\delta} \partial T_e / \partial y$ and $e^{-1} n_e^{-1} j_{y\delta} \partial p_e / \partial y$ in the right side of the electron energy equation (1.4), which describe the transport of electron enthalpy by the electric current and the work done by the electron pressure, have different signs in the anode and cathode boundary layers: the upper sign corresponds to the anode, and the lower sign to the cathode. We consider the following boundary conditions:

$$\begin{gathered} v_x = v_y = 0, \quad T_i = T_{iw}, \quad T_e = T_{ew} \quad (y = 0) \\ v_x = v_{x\delta}, \quad T_i = T_{i\delta}, \quad T_e = T_{e\delta} \quad (y \to \infty) \end{gathered} \tag{1.6}$$

For transfering (1.1)-(1.5) to dimensionless form, we use the following parameters: the ratio of the ion mass to the proton mass $m = m_i/m_p$, the Coulomb logarithm at the input to the channel λ_0, load factor K, the load parameter S, and also the Mach M_0, Reynolds R, and Hall Ω_0 numbers:

$$K = \frac{cE_{y\delta}}{v_0 H}, \quad S = \frac{\sigma_0 H^2 L}{c^2 \rho_0 v_0}, \quad M_0 = \sqrt{\frac{3\rho_0 v_0^2}{5 p_0}}, \quad R = \frac{\rho_0 v_0 L}{\mu_i^\circ}, \quad \Omega_0 = \frac{eH\tau_e^\circ}{m_e c}$$

It is assumed that all quantities vary only with the longitudinal coordinate x in the body of the flow. In calculating the distributions of the gas-dynamic parametes $v_{x\delta}$, $T_{i\delta}$, $T_{e\delta}$, and p_δ and the current density $j_{y\delta}$ in the external flow, we omit in (1.1)-(1.4) all derivatives with respect to y and use one-dimensional theory. It can easily be shown that the change in the velocity and Mach number along the channel are then given qualitatively by the Resler–Sears diagram [8]. In integrating the one-dimensional system it is assumed that the component temperatures, velocity, and the density at the input to the channel are given.

We have considered subsonic and supersonic conditions for the MHD channel with the energy supplied to the flow in such a way that acceleration occurs with simultaneous increase in the Mach number. It follows from the Resler–Sears diagram that for subsonic flow with fixed M_0 and K the value of S cannot exceed somce critical value which is determined by the cut-off condition M = 1 at x = L. Calculations were carried out for a lithium plasma so that m = 6.8849. Subsonic flow was considered for the following parameter values:

$$\begin{gathered} T_e^\circ = 10\,000^\circ \text{ K}, \quad T_i^\circ = 5000^\circ \text{ K}, \quad n_i^\circ = 10^{15} \text{ cm}^{-3}, v_0 = 4 \cdot 10^5 \text{ cm/sec} \\ H = 100 \text{ G}, \quad E_{y\delta} = 1.65 \text{ V/cm}, j_y^\circ = 36.9 \text{ A/cm}^2 \end{gathered} \tag{1.7}$$

which correspond to

$$M_0 = 0.7306, \quad K = 4.136, \quad \Omega_0 = 0.0944, \quad \lambda_0 = 5.1338.$$

Cut-off occurred at a length L = 3.5 cm and was obtained at S = 0.2242, R = 8112. The calculations for the supersonic flow were made with

$$\begin{gathered} T_e^\circ = 10000^\circ \text{ K}, \quad T_i^\circ = 2500^\circ \text{ K}, \quad n_i^\circ = 10^{14} \text{ cm}^{-3} \quad v_0 = 10^6 \text{ cm/sec} \\ H = 100 \text{ G}, \quad L = 11.3 \text{ cm}, \quad E_{y\delta} = 1.1, 1.5, 1.8 \text{ V/cm} \\ j_y^\circ = 2.6, 12.9, 20.6 \text{ A/cm}^2 \end{gathered} \tag{1.8}$$

TABLE 1

ξ	q_e, kW/m²				$\lvert q_j \rvert$, kW/m²		q_i, kW/m²			
Variant	A2	C2	A6	C6	C2	C6	A2	C2	A6	C6
0	—	—	—	—	460.54	286.42	—	—	—	—
0.01	−1054.58	829.48	−993.11	909.09	380.19	302.53	−12.02	5.48	−15.54	4.37
0.1	−338.49	127.36	−1552.59	814.75	311.93	318.18	−15.51	8.98	−12.88	1.58
0.2	−336.56	94.06	−1995.00	1147.07	321.69	307.04	−16.26	8.07	−12.08	1.46
0.3	−355.30	78.42	−1637.11	1040.10	331.10	178.90	−16.70	7.93	−8.48	2.59
0.4	−381.75	68.98	−1189.31	826.06	339.88	97.52	−17.48	7.81	−6.54	3.73
0.5	−412.09	62.86	−876.82	652.83	347.91	54.22	−18.45	7.73	−5.86	4.41
0.6	−444.23	57.37	−665.96	518.96	355.13	31.25	−19.49	7.67	−5.69	4.91
0.7	−477.20	53.16	−521.79	420.18	361.48	18.66	−20.55	7.63	−5.72	5.24
0.8	−510.63	50.22	−419.68	345.64	367.00	11.49	−21.63	7.61	−5.83	5.51
0.9	−545.47	47.90	−345.06	288.84	372.20	7.27	−22.72	7.56	−5.97	5.73
1.0	−595.97	48.45	−289.16	244.88	382.36	4.71	−23.87	7.25	−6.11	5.92

which correspond to

$$M_0 = 2.0009,\ S = 2.3036,\ \Omega_0 = 0.8285,\ \lambda_0 = 5.8473,$$
$$R = 42073,\ K = 1.1,\ 1.5,\ 1.8.$$

2. Results of the Calculations

The system (1.1)-(1.6) was solved by the iterative method of successive passes [9]; we used the Dorodnitsyn variables

$$\xi = \frac{x}{L}, \quad \eta = \sqrt{\frac{\rho_0 v_0}{\mu_i^\circ x}} \int_0^y \frac{n_i}{n_{i\delta}}\, dy \tag{2.1}$$

The boundaries layers were studied at the anode (variants A1, A2, A3, A4, A5 and A6) and at the cathode (variants C2 and C6). The values given in (1.7) and (1.8) were taken as characteristic values for the input to the channel. At the walls we considered the following conditions: $T_{iw} = 1250°K$, $T_{ew} = 5000°K$ for variants A1, A3, A4 and A5; $T_{ew} = T_{iw} = 4500°$ for variants A2 and C2; $T_{iw} = 1000°K$, $T_{ew} = 5000°K$ for variants A6 and C6. For A1, A2 and C2, the flow was subsonic with $K = 4.136$ and in the remaining variants it was supersonic with $K = 1.1$ (A3), $K = 1.5$ (A4) and $K = 1.8$ (A5, A6 and C6).

Estimates show [10] that in a fully ionized two-temperature plasma the thickness of the temperature boundary layer of electrons δ_e is considerably greater than the thickness for a viscous or an ion temperature boundary layer. For this reason the asymptotic boundary condition (1.6) was applied in the calculations at the external boundary of the electron temperature boundary layer. The value of δ_e was determined from the condition that there should be a smooth transition from the electron temperature profile in the boundary layer to the electron temperature distribution along the channel $T_{e\delta}^{-1} \partial T_e / \partial \eta = 10^{-2}$ at $\eta = \delta_e$. In the variables (2.1), we get $\delta_e = 24$. Figure 1 shows the initial parts of the component temperature profiles at the cross section $\xi = 0.5$ when the flow round the electrodes is subsonic. It can be seen that when the component temperatures at the wall are different (A1), relaxation of the temperature difference $T_{ew} - T_{iw}$ created at the wall occurs in a thin layer near the wall – the δ-layer [10, 11]. The nature of the temperature variation in the δ-layer is quite different for the two components: the ion temperature increases sharply away from the wall whereas the electrom temperature is almost constant.

The formation of the δ-layer is brought about by two factors: the interchange of energy between the components and the equalization of the ion temperature as a result of thermal conductivity. If, however, $T_{ew} = T_{iw}$, so that there is little energy interchange near the wall (A2 and C2 in Fig. 1), then there is no δ-layer. Then as a result of viscous heating of the ion gas at the electrode surface $T_i > T_e$. A comparison of profiles for the same component temperatures at the two electrodes (A2 and C2) shows that as a result of the diffusion of electron enthalpy and the work done by electron pressure forces during the current flow, the temperatures T_e and T_i in the boundary layers are higher at the anode than at the cathode. The term describing the viscous heating in the energy equation for the ion gas is proportional to M^2, and therefore there is a considerably more intensive heating of the ions near the walls under supersonic channel operation than with subsonic flow. Thus the calculation for variant A3 which has the same values of T_{ew} and T_{iw} as A1 shows

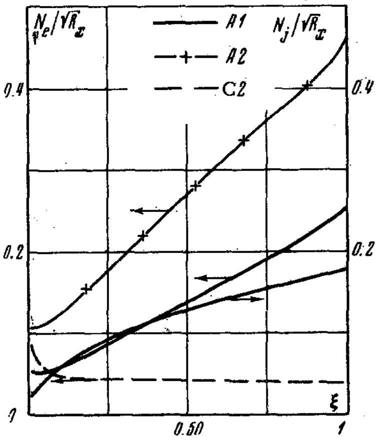

Fig. 2

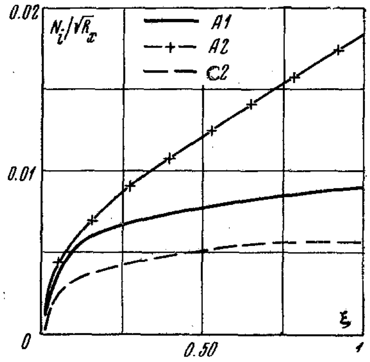

Fig. 3

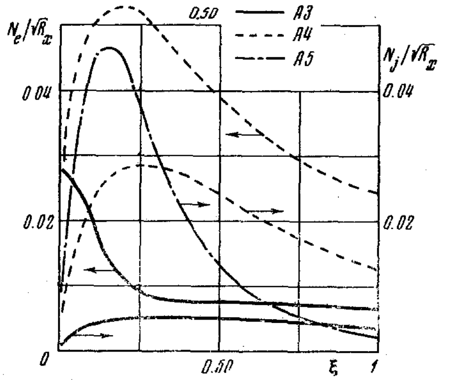

Fig. 4

that the ion temperature is higher than the electron temperature for some distance from the walls in the viscous boundary layer.

An analysis established that the partial pressures varied sharply across the δ-layer with the electron pressure falling and the ion pressure increasing from the wall and the overall pressure p remaining constant. Since p does not vary across the channel and the pressure near the walls is lower than that in the bulk flow, the density in the boundary layers is higher than in the external flow. Calculations show that at fixed K and $M_0 > 1$ the density near the wall decreases more rapidly away from the input to the channel than the flow accelerating force $f = c^{-1}j_{y\delta}H - dp_\delta/dx$ increases. Thus the velocity gradient $\partial v_x/\partial\eta$ near the wall increases with ξ and the viscous heating of the ions becomes greater. If the load coefficient is increased (variants A3, A4, and A5), the current density and therefore the Joule heating increase so that the electron temperature in the bulk flow goes up. The temperature drop $T_{e\delta} - T_{ew}$ across the boundary layer increases as does the gradient $(\partial T_e/\partial\eta)_w$.

The temperature and current density distributions that were obtained were used to calculate the dimensional energy fluxes (kW/m²) q_e, q_i, and q_j to the electrodes caused by the electron and ion thermal conductivities and also by the transport of electron enthalpy by the electric current and the diffusion of electrons in the magnetic field:

$$q_e = -\varkappa_{ew}\left(\frac{\partial T_e}{\partial y}\right)_w, \quad q_i = -\varkappa_{iw}\left(\frac{\partial T_i}{\partial y}\right)_w, \quad q_j = -\frac{3.211}{e} j_{y\delta} T_{ew}$$

The velocity and density profiles were used to determine the displacement thickness

$$\delta^* = \int_0^\infty \left(1 - \frac{\rho v_x}{\rho_\delta v_{x\delta}}\right) dy = \sqrt{\frac{x\mu_i^\circ}{\rho_0 v_0}} \int_0^\infty \frac{n_{i\delta}}{n_i}\left(1 - \frac{n_i v_x}{n_{i\delta} v_{x\delta}}\right) d\eta$$

We also calculated the dimensionless parameters characterizing the friction and thermal exchange at the electrodes – the coefficient of friction c_f and Nusselt numbers N_e, N_i and N_j; these are related to the corresponding energy fluxes by the equations

$$c_f = \frac{2\mu_{iw}(\partial v_x/\partial y)_w}{\rho_\delta v_{x\delta}^2} = \frac{2}{R_x^{1/2}} \frac{n_{iw}}{n_{i\delta}} \frac{T_{iw}^{5/2}}{(T_i^\circ T_{i\delta})^{5/4}} \frac{(\lambda_0\lambda_\delta)^{1/2}}{\lambda_w v_{x\delta}} \left(\frac{\partial v_x}{\partial\eta}\right)_w$$

$$N_k = \frac{2.5 q_k x}{m_i \varkappa_{ew}(h_\delta - h_w)}, \quad R_x = \frac{\rho_\delta v_{x\delta} x}{\mu_{i\delta}}, \quad h = \frac{5}{2}\frac{p}{\rho} + \frac{v_x^2}{2}$$

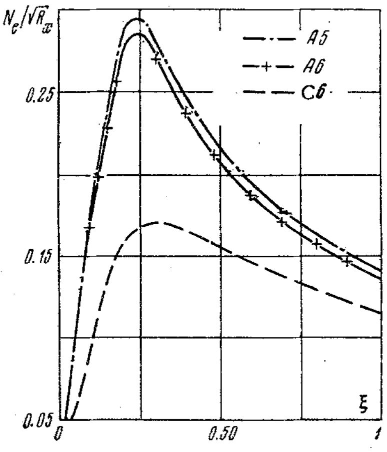

Fig. 5

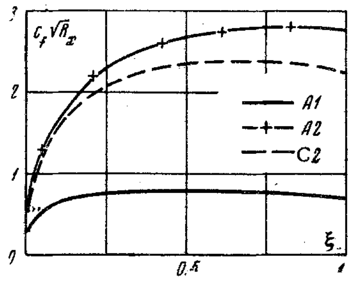

Fig. 6

TABLE 2

ξ	$\delta^* (\rho_0 v_0)^{1/2} (x\mu_i{}^\circ)^{-1/2}$		
Variant	A3	A4	A5
0	1.4578	1.4578	1.4578
0.01	0.4773	1.3622	2.2574
0.1	0.5160	0.5961	1.3188
0.2	0.3717	0.4239	0.9002
0.3	0.3223	0.3450	0.5451
0.4	0.2889	0.3007	0.3652
0.5	0.2650	0.2750	0.2839
0.6	0.2465	0.2562	0.2427
0.7	0.2320	0.2425	0.2199
0.8	0.2202	0.2320	0.2048
0.9	0.2104	0.2235	0.1935
1.0	0.2020	0.2163	0.1842

where R_x is the actual Reynolds number and h is the sum of the enthalpy per unit mass and the kinetic energy density.

Figures 2-5 show the distributions of the parameters $N_e/\sqrt{R_x}$, $N_i/\sqrt{R_x}$, $N_j/\sqrt{R_x}$ along the electrodes for various operational conditions in the MHD channel. The values of the energy fluxes give an idea of the intensity of the heating which occurs at the anode and the cathode and are given in Table 1. An analysis of the results shows that at a sufficiently high current density (subsonic conditions) the diffusion of electron enthalpy and the work done by the electron pressure forces during the current flow play a significant part in the energy balance in the boundary layer so that the heat fluxes q_e and q_i are several times greater at the anode than at the cathode. It should be noted that despite the fact that $(\partial T_i/\partial y)_w \gg (\partial T_e/\partial y)_w$, the high thermal conductivity of the electrons means that $q_e > q_i$. In contrast to the heat fluxes from thermal conductivity, which are directed towards the electrodes, the electric current carries electron enthalpy from the cathode to the anode and thus the heating at the anode is increased and that at the cathode is decreased. If the current density is increased (it is assumed that the mechanism determining the production and loss of charged particles at the electrodes surfaces allows $j_{y\delta}$ to be increased), the energy flux q_j goes up. With the flow parameters used here, $|q_e + q_i| < |q_j|$ for subsonic flow and $|q_e + q_i| > |q_j|$ for supersonic flow.

In supersonic flow there is intensive heating of the electron component in the γ-layer as the load coefficient increases [12]. As a result of this, the electron temperature drop across the boundary layer over the initial parts of the electrodes increases with K. The electron heating also produces a sharp rise in the conductivity so that for large K there is a localized current of increased density in the γ-layer. Thus under supersonic conditions the distributions of q_e, q_j, $N_e/\sqrt{R_x}$, $N_j/\sqrt{R_x}$ have maxima in the initial part of the flow. Since the component temperatures are higher in the boundary layers at the anode on account of the diffusion of electron enthalpy and the pressure of the mixture does not change across the channel, the density is greater near the anode than near the cathode. For the same force f the gas at the anode undergoes a greater acceleration than does that at the cathode. Thus the friction forces are greater at the anode than at the cathode; this result is in agreement with the calculated distribution of the quantity $c_f\sqrt{R_x}$ along the electrodes shown in Figs. 6 and 7.

The localization of the electric current in the γ-layer produces an increase in the Lorentz force in the initial part of the flow and a drop in density near the anode; this explains the presence of the maxima in $c_f\sqrt{R_x}$ when the flow past the anode is supersonic.

The value of the dimensionless displacement thickness at various cross sections in the channel (normalized by $(x\mu_i{}^\circ)^{1/2}(\rho_0 v_0)^{-1/2}$) is shown in Table 2. Using these data we can easily show that δ^* in the developed flow is of the order of several ion mean free paths under the same conditions already considered. We may note that because the Prandtl number of the electron component

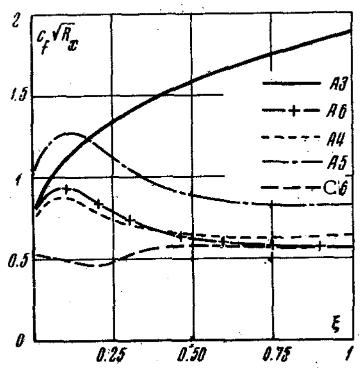

Fig. 7

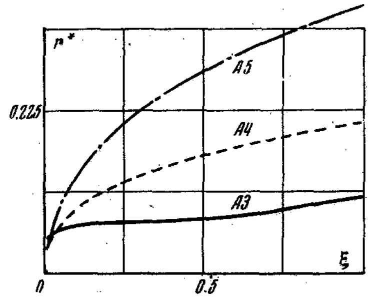

Fig. 8

$$Pr_e = 2.5\varkappa_e^\circ / (m_i\mu_i^\circ) \sim (m_e / m_i)^{1/2} (T_i^\circ / T_e^\circ)^{5/2}$$

is small, the thickness of the electron temperature boundary layer is much greater than δ^*.

In order to estimate the effect of the boundary layers on the external flow, it is of interest to consider the magnitude of the ratio $r^* = r_c/r_i$ of the electrical resistance of the boundary layers at the electrodes (r_c) to the internal resistance of the MHD channel (r_i) when the boundary layers are neglected:

$$r_c = 2 \int_0^{\delta_e} \sigma^{-1} dy, \quad r_i = a/\sigma_\delta \tag{2.2}$$

where a is the distance between the electrodes. The first equation in (2.2) is not useful in studying the asymptotic boundary layers because $r_c \to \infty$ as $\delta_e \to \infty$. Thus the parameter characterizing the resistance of the boundary layers should be taken as

$$r_c = \lim_{\delta_e \to \infty} 2 \int_0^{\delta_e} \left(\frac{1}{\sigma} - \frac{1}{\sigma_\delta}\right) dy = 2L \sqrt{\frac{\xi}{R}} \int_0^\infty \frac{n_{i\delta}}{n_i} \left(\frac{1}{\sigma} - \frac{1}{\sigma_\delta}\right) d\eta$$

which is bounded as $\delta_e \to \infty$. The extra term is of the order of σ_c/σ_δ, where σ_c is a characteristic value of the conductivity near the electrodes. Distributions of r^* as a function of ξ for various values of K are given in Fig. 8; the value of L/a was taken as 10. Since the electron gas in heated more strongly in the bulk flow than in the boundary layers as the load coefficient increases, the resistance of the channel decreases with rise in K, and the value of r^* goes up.

The author thanks V. V. Gogosov and A. E. Yakubenko for interest in this work.

LITERATURE CITED

1. S. I. Braginskii, "Transport phenomena in a plasma," in: Problems in Plasma Theory [in Russian], No. 1, Atomizdat, Moscow (1963).
2. V. V. Gogosov and V. M. Korovin, "The solution of the boundary layer equations at the electrodes in a fully ionized plasma with different component temperatures," Izv. Akad. Nauk SSSR, Mekhan. Zhidk. i Gaza, No. 5 (1970).
3. L. E. Kalikhman, "The boundary layer of a two-temperature plasma at the electrodes of a magnetohydrodynamic channel with crossed electric and magnetic fields at high values of the Hall parameter," Zh. Prikl. Mekh. i Tekh. Fiz., No. 3 (1969).
4. L. E. Kalikhman, "An approximate method for calculating the boundary layer of a two-temperature plasma at the electrodes with high values of the Hall parameter," Zh. Prikl. Mekh. i Tekh. Fiz., No. 1 (1970).
5. G. C. Oates, J. K. Richmond, Y. Aoki, and G. Grohs, "Loss mechanisms of a low-temperature plasma accelerator," JARS, 32, No. 4 (1962).
6. V. V. Proshkin, "The boundary layer of a weakly ionized gas at the electrodes of a MHD channel with allowance for the electron temperature runaway," in: Problems in the Physics of a Low-Temperature plasma [in Russian], Nauka i Tekhnika, Minsk (1970).

7. H. A. Claassen, "The laminar magnetogasdynamic electrode boundary layer of a thermal nonequilibrium plasma," Electricity from MHD, Vol. 4, Vienna (1968).
8. E. L. Resler, Jr., and W. R. Sears, "The prospects for magnetoaerodynamics," J. Aeronaut. Sci., 25, No. 4, 235 (1958).
9. I. Yu. Brailovskaya and L. A. Chudov, "The solution of the boundary layer equations by a difference method," in: Numerical Methods and Programming [in Russian], 1st ed., Izd-vo MGU, Moscow (1962).
10. V. V. Gogosov, "Boundary layers in a fully ionized two-temperature plasma," Prikl. Matem. i Mekhan. 30, No. 3 (1966).
11. V. V. Gogosov, "The boundary layers in a two-temperature plasma," in: Electricity from MHD, Vol. 2, Vienna (1966).
12. V. M. Korovin, "Studies of the boundary layers of a fully ionized two-temperature plasma at a nonconducting wall in a MHD channel," Izv. Akad. Nauk SSSR, Mekhan. Zhidk. i Gaza, No. 5 (1972).